Journal of Alloys and Compounds 509 (2011) 7193–7197

Contents lists available at ScienceDirect

Journal of Alloys and Compounds

journal homepage: www.elsevier.com/locate/jallcom

Effects of post-annealing on Schottky contacts of Pt/ZnO films toward UV photodetector

Y.Z. Li[a,b], X.M. Li[a,*], X.D. Gao[a]

[a] State Key Laboratory of High Performance Ceramics and Superfine Microstructures, Shanghai Institute of Ceramics, Chinese Academy of Sciences, Shanghai 200050, People's Republic of China
[b] Graduate School of Chinese Academy of Sciences, Beijing 100039, People's Republic of China

ARTICLE INFO

Article history:
Received 3 December 2010
Accepted 1 April 2011
Available online 22 April 2011

Keywords:
ZnO films
Post-annealing
Schottky contact
UV photodetector

ABSTRACT

The Schottky contact of Pt/ZnO was formed by depositing ZnO films oriented along *c*-axis by pulsed-laser deposition on Pt/Ti buffer layer supported by SiO_2/Si substrate. Effects of the post-annealing on the crystallinity, uniformity and native defects of ZnO film as well as Schottky contacts of Pt/ZnO films were investigated. Results show that the annealing can improve the crystallinity of ZnO film, suppress the native defects, and enhance the performance of Pt/ZnO Schottky contacts dramatically. The best Schottky diode shows the largest barrier height of 0.8 eV with reverse leakage current of 1.5×10^{-5} A/cm^2. The zero-biased photodetector based on the best Schottky diode possesses responsivity of 0.265 A/W at 378 nm, fast photo-response component with rise time of 10 ns and fall time of 17 ns. This report demonstrates possibility of ZnO films/Pt hetero-junction with large area Schottky contact, and establishes the potential of this material for use in UV photodetector devices.

1. Introduction

ZnO is an attractive material for use in ultraviolet optoelectronic devices due to its physical properties, such as direct wide band gap of 3.37 eV or large exciton binding energy of 60 meV at room temperature [1–3]. Many methods have been used to grow ZnO thin films such as pulsed laser deposition (PLD), and have been proven successful in growing ZnO films with high crystalline quality [4–6]. For ZnO films used in LEDs or photodetector, not only the high crystalline quality of films, but also the electrical characterization of the contacts formed by various metal or alloys to ZnO is desired. Several groups have reported the Schottky contact on ZnO crystal [7–13] fabricated by using Pd, Au and Ag as Schottky metals, but the studies of Pt/ZnO films Schottky contact through finding a sub-layer which would allow ZnO films re-growth were relative rare.

Earlier work on the growth of ZnO thin films on Pt layers mainly focused on its oxidation resistance and low vapor pressure even at high temperatures [14–17]. These authors indicate good epitaxial quality of the ZnO material as measured by RHEED and X-ray diffraction (XRD). However, there is no report on the effects of post-annealing on electrical properties of Pt/ZnO contacts through deposition of ZnO films on Pt/Ti buffer layers. In addition, Pt metal forms a Schottky contact with n-type ZnO. Thus, ZnO/Pt heterostructures may offer a range of advantages for the realization of optoelectronic devices such as ultraviolet photodetectors. The electrical properties of Pt/ZnO film contacts is a key to the use of ZnO films in such devices and a study of such properties is vital in determining the potential of such heterostructure for device applications.

The main aim of the present paper is to systematically study the effects of post-annealing on crystalline quality, uniformity of ZnO films, modification of native defects in ZnO films and the electrical properties of Pt/ZnO thin films contacts, and explore the potential application of the contact in zero-biased photodetector.

2. Experimental details

Before deposition of platinum layer about 200 nm thick with a homogeneous and smooth morphology on SiO_2/Si substrate, titanium layers with thickness of 20 nm were inserted to augment the adhesion between platinum layer and substrate. These samples were then transferred in air to the PLD chamber. ZnO films were grown by PLD (Lambda Physik COMpex) on Pt/Ti/SiO_2/Si substrate at 300 °C, in an oxygen pressure of 2 Pa. 120 min were required to grow films with thickness of about 250 nm. Post-annealing was performed at temperature of 400 °C, 500 °C, 600 °C, 700 °C and 800 °C for 1 h at air, respectively. After the growth of films, the Pt/Ti alloy (25/20 nm) used as ohmic electrode (200 μm diameter) was patterned on top of ZnO films via shadow mask by electrical beam evaporation. Pt bottom layer was expected as electrode of Schottky contacts, and the deposited Pt/Ti double layer on top of films as electrode of ohmic contacts. The crystallinity, interface and surface morphology of ZnO films were characterized by X-ray diffraction (XRD, Bruker-AXS), scanning electron microscopy (SEM, JSM-6700F) and atomic force microscopy (AFM, Seiko SPA300HV), respectively. The photoluminescence (PL) spectra of the ZnO films were measured at room temperature (RT) using the 325 nm line of a continuous

* Corresponding author. Tel.: +86 021 52412554; fax: +86 021 52413122.
E-mail addresses: lixm@mail.sic.ac.cn, xdgao@mail.sic.ac.cn, leeyuntse@sina.com (X.M. Li).

0925-8388/$ – see front matter.
doi:10.1016/j.jallcom.2011.04.039

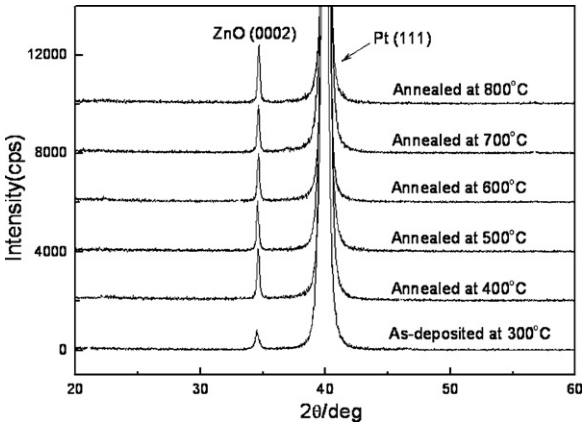

Fig. 1. XRD patterns of ZnO films.

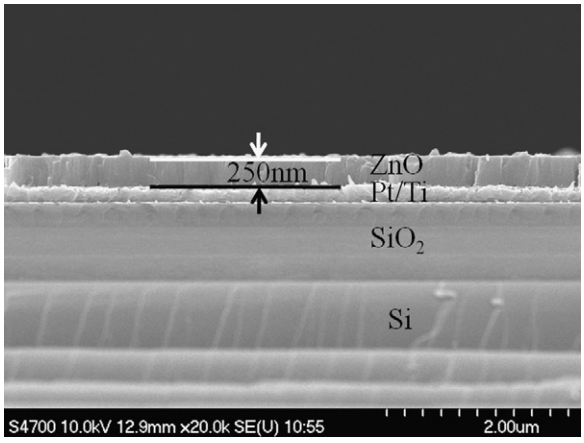

Fig. 2. Cross sectional SEM of ZnO film (post-annealed at 600 °C).

wave He–Cd laser (PL, Jobin Yvon LabRAM HR 800UV micro-Raman system). *I–V* measurements were carried out in semiconductor characterization system (Keithley 4200-SCS). The spectral response was carried out using a 150 W Xe arc lamp and a monochromator. The incident power on the sample was calibrated using a commercial UV enhanced Si photodiode, from which the responsivity values were obtained.

3. Results and discussion

Fig. 1 displays a typical XRD pattern for the ZnO films deposited on Pt buffer layer, which shows that the ZnO films are purely *c*-axis oriented. With the increase of the annealing temperature, the FWHM of the XRD decreases from 0.454 to 0.198, showing the release of the strain in the film and the improvement of crystallinity through post-annealing at air. Fig. 2 shows the cross-sectional SEM image of films deposited at 300 °C on Pt buffer layer. It can be seen that the obtained film possesses a homogeneous columnar crystalline structure with a thickness of about 250 nm. Fig. 3 shows the AFM image of ZnO films. It can be seem from the planar description that ZnO films present larger and denser grain after post-annealing, which is consistent with the results obtained from XRD.

Fig. 4 shows the room temperature PL spectrum. It is clear that the near band edge (NBE) emissions of ZnO films were located at wavelength of 378 nm. As FWHM of NBE emission of ZnO films is closely related to the crystalline quality, the narrow width and high intensity give clear evidence that post-annealing temperature take great effects upon the crystalline quality of ZnO films. It can be seen that the NBE emission intensity of as-deposited film increases and the FWHM of the NBE emission decrease from 14.51 nm to 12.24 nm with the increase of annealing temperature, which is also consistent with XRD analysis. There is weak emission peak corresponding to any defects in the case of as-deposited film between the wavelength of 450 nm and 700 nm. After post-annealing at temperature from 400 °C to 700 °C, the variation of emission intensity related to defects is tiny. The emission intensity ratio of $I_{NBE}/I_{520\,nm}$ increases from 17.7 to 991.8, which indicates that the defects (may be oxygen vacancy) in ZnO films can be reduced by the post-annealing

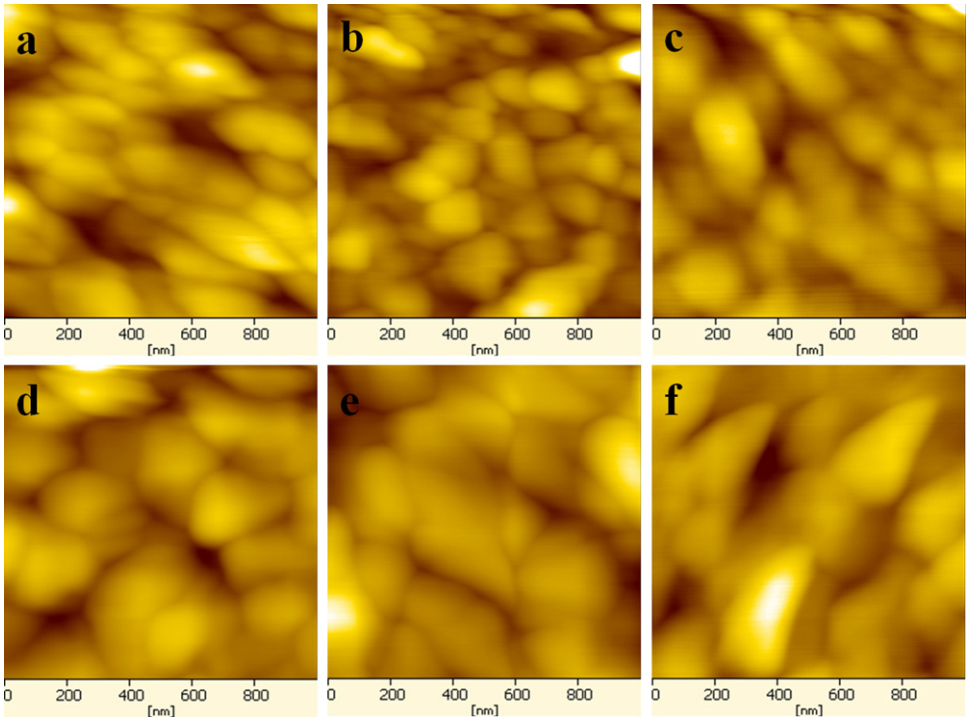

Fig. 3. AFM image of ZnO films.

Table 1
Performance parameters of ZnO films and related diodes.

Conditions	I_{NBE}/I_{520}	O/Zn ratio	I_{2v}/I_{-2v}	I_R (A)	φ_B (eV)	Ideality (n)
As-deposited	17.7	0.93	11	0.021	>0	–
Annealed at 400 °C	317.6	0.95	78	1.2×10^{-3}	0.65	2.96
Annealed at 500 °C	394.5	0.98	115	2.06×10^{-4}	0.74	2.84
Annealed at 600 °C	856.4	0.99	1220	1.5×10^{-5}	0.80	2.33
Annealed at 700 °C	991.8	1.02	8	1.8×10^{-3}	>0	–
Annealed at 800 °C	153.8	1.06	1	0.41	0	–

(shown in Table 1). However, as the annealing temperature further increase, the emission peak corresponding to defects between the 450 nm and 700 nm suddenly increase, and the emission intensity ratio of $I_{NBE}/I_{520\,nm}$ decrease to about 153.8. It may be resulted from decomposition of ZnO film at high temperature of 800 °C. Thomas found that Zn evaporate readily in a Zn-poor environment, even at low temperatures or annealing for several hours [18]. As the annealing temperature arrives at 800 °C, the decomposition happens, which may lead to more defects in ZnO films such as V_O and V_{Zn}.

Fig. 5(a) shows the auger energy spectrum analysis of ZnO film near ZnO/Pt interface layer (located at depth of 210 nm from ZnO surface). At the kinetic energy of 200 eV, there exist a weak peak corresponding to C element. It may be formed during process of transferring Pt buffer layer from sputtering chamber to PLD chamber. Near the kinetic energy of 380 eV, the peak corresponding to Ti element appears after the post-annealing above 700 °C. It may be resulted from the thermal diffusion of Ti from Ti adhesion layer into ZnO films. Compared with the relative weak peak, the peak corresponding to O and Zn are much stronger. It can be observed from Fig. 5(b) that the O/Zn ratio varies with depth from ZnO film surface. As the annealing temperature increases, the variation of O/Zn ratio becomes smooth, which indicates that the films were prone to be uniform after post-annealing. As the post-annealing temperature below 600 °C, the average O/Zn ratio increases with the increase of annealing temperature. But when the annealing temperature arrives at 700 °C, the O/Zn ratio shows little more than 1:1. It may be due to the exceeded oxygen absorbed by diffused Ti. Table 1 shows the average O/Zn ratio of ZnO films annealed at different temperature. When the annealing temperature is improved, which indicates that the post-annealing could suppress the O vacancy. However, the O/Zn ratio suddenly arrives at 1.06 when the annealing temperature was 800 °C, which may be resulted from the evaporation of Zn from ZnO film. On the other hand, it also could be due to the exceeded oxygen absorbed by diffused Ti from the Ti adhesion layer. It can be assumed that the native defects V_{Zn} and V_O could be formed in the ZnO film annealed at 800 °C while V_O exists in the ZnO films annealed below 800 °C.

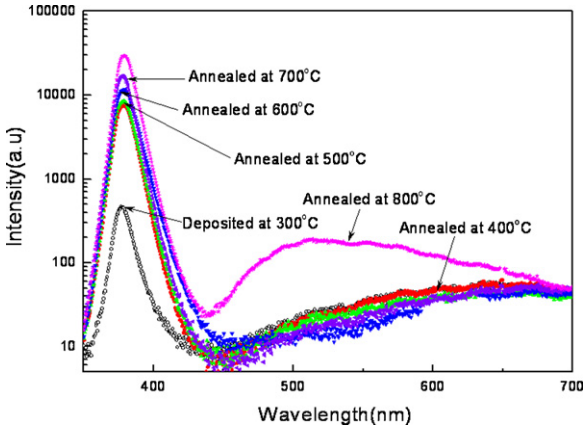

Fig. 4. Photoluminescence spectrum of ZnO films.

Fig. 6(a) shows monotonic changes from ohmic to Schottky behavior. Schottky barrier and ideality factors were extracted from current–voltage using thermionic field emission analysis based on Eqs. (1) and (2). S represents the Schottky contact area (about 1 cm^2).

$$I = I_0 \exp\left[\left(\frac{qV}{nkT}\right) - 1\right] \quad (1)$$

$$I_0 = SA^{**}T^2 \exp\left(-\frac{q\phi_B}{kT}\right) \quad (2)$$

It is evident that as-deposited film diode has non-ideal rectification behavior. With the increasing of the annealing temperature below 600 °C, the Schottky rectification of diode is declined to be more and more evident, and the forward–reverse current (I_{2v}/I_{-2v}) suppression ratio is from 11 to 1220. It may be resulted from the improvements of crystalline quality, suppression of deep level defects and better interface with less dislocation after post-annealing. However, the diode based on ZnO film annealed at 700 °C shows bad rectification behavior, the forward–reverse current suppression ratio is dramatically reduced to 8. As the annealing temperature was 800 °C, the diode deteriorated substantially, and

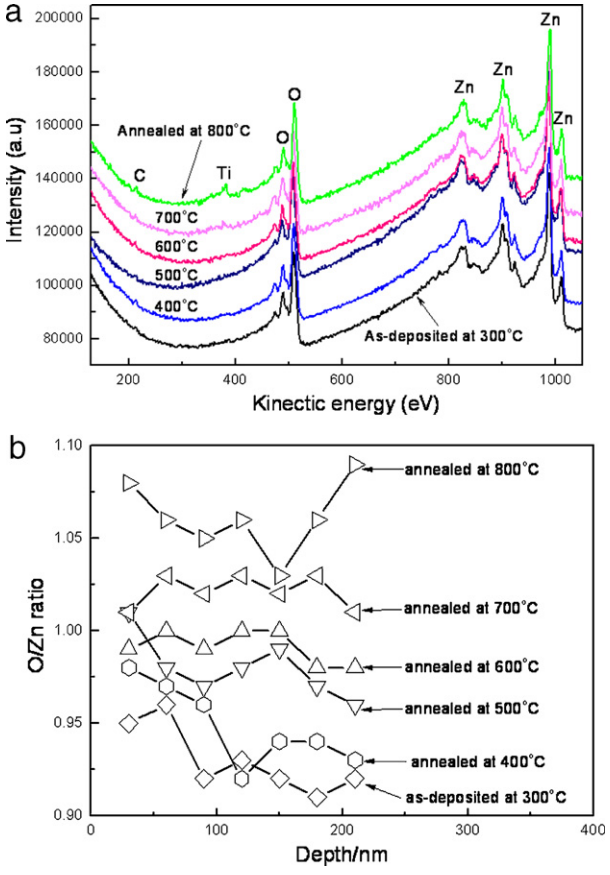

Fig. 5. (a) Auger energy spectrum of ZnO films. (b) O/Zn ratio as a function of depth from ZnO film surface.

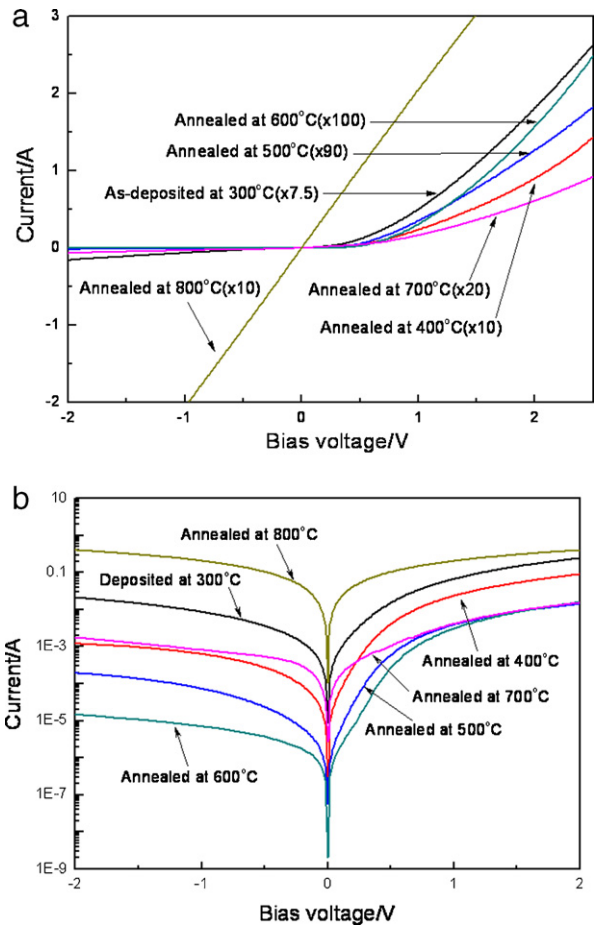

Fig. 6. (a) *I–V* characteristics of Schottky diodes based on ZnO films. (b) Reverse leakage current of Schottky diodes.

the Pt/ZnO contact was transferred from Schottky to ohmic contact. The result seems to be contradictory with XRD analysis and PL spectrum, which may be due to the Ti diffusion from adhesion layer when ZnO films were annealed at 700 °C. The Ti element at the Pt/ZnO film interface may form ohmic contact with ZnO film as a results of its low work function. Thus, the electron tunnel-like penetration effects lead to the reduction of barrier height. As ZnO films were annealed at 800 °C, the Ti content at interface increase, and a thin Ti layer may be formed between Pt and ZnO film. The contacts between Pt and ZnO film was actually dominated by the contacts between Ti thin layer and ZnO film. Thus, the *I–V* curve shows ohmic behavior. The estimated barrier height and the ideality factor for fabricated Schottky diodes are labeled in Table 1. The barrier height of diode based on ZnO films annealed at 400 °C, 500 °C and 600 °C are 0.65 eV, 0.74 eV and 0.79 eV, while the ideality factor is on the decrease. The barrier height and ideality of diode based on films deposited at 300 °C, annealed at 700 °C were difficult to be estimated accurately as a results of no evident linear part in *I–V* curve (shown in Fig. 6(b)). But it can be assured that the barrier height was above zero and improved by post-annealing because reverse current are related to barrier height based on Eq. (2). Fig. 6(b) shows the reverse leakage current I_R of obtained Schottky diode. It decreases by over three orders of magnitude through the simple post-annealing, which reflects the improvement of barrier height in turn.

The diode was illuminated by light at wavelength ranging from 300 nm to 700 nm. The light power of the illuminated light at wavelength of 368 nm is 0.95 μW. The photo-response spectrum of diode is shown in Fig. 7. The diode based on ZnO films annealed at 500 °C

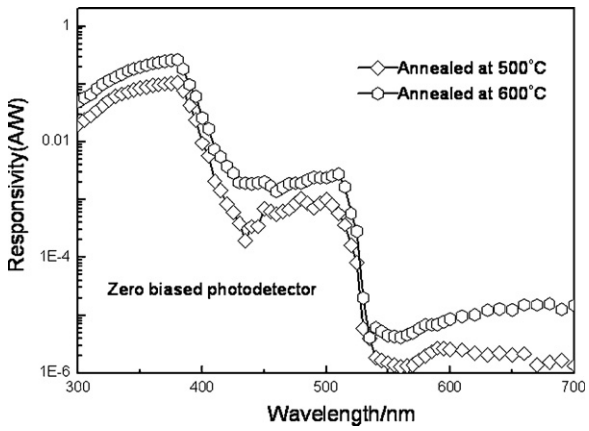

Fig. 7. Spectral photoresponse of Schottky diode illuminated by light.

and 600 °C show photo-response, but there is no evident photo-response for other diode (not displayed in Fig. 7). This phenomenon could be due to the substantial recombination of photo-induced electron–hole pairs in depletion layer. For the as-deposited film, there exist defects such as dislocation and V_O which could act as center of recombination. On the other hand, the internal built electrical filed (or barrier height) is weak. Although the annealing at 400 °C could improve the crystalline quality of ZnO film and the barrier height can be improved, there still exist enough defects (reflected by the reverse leakage current) which could trap photo-induced electrons. As the annealing temperature further increases to be 500 °C, the barrier height can be further improved and the defects could be reduced so enough as the photo-induced electron could be pulled out under force of in-built electrical field. As the annealing temperature arrives at 600 °C, the barrier height and defects could be further modified, which may lead to more photocurrent or evident photo-response. In Fig. 7, it can be seen the responsivity shows ladder-shaped change. The peak responsivity corresponding to the film annealed at 500 °C is about 0.105 A/W, and that corresponding to the film annealed at 600 °C is 0.265 A/W. It decreases sharply at wavelength of 378 nm and 520 nm. The sharp cut-off at wavelength of 378 nm agrees with ZnO film energy band gap of 3.28 eV. The photo-response between wavelength of 420 nm and 520 nm may be due to the exciton weak tied by deep level defects such as V_O, while that between 520 nm and 700 nm could be resulted from the background noise of measurement system. In order to study the photo-response speed of fabricated diode, the KrF excimer laser with wavelength of 248 nm was used for pulsed light

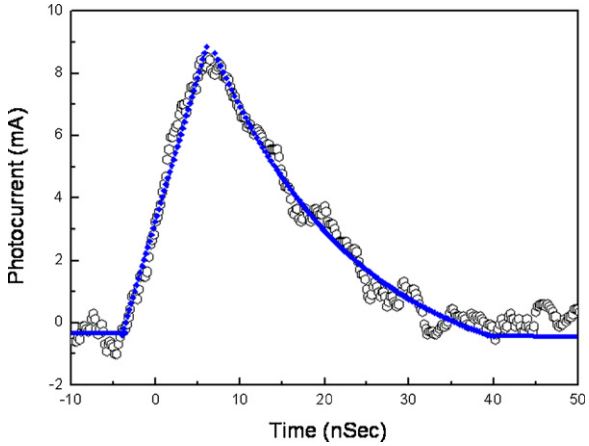

Fig. 8. Photocurrent as a function of response time of photodetector.

resource. The pulse width was 60 ns and the energy of 20 mJ/pulse was weakened to prevent the film from damaging. Fig. 8 shows the photocurrent as a function of time from photodetector based on ZnO film annealed at 600 °C. The photo-response has fast component which rises within 10 ns and falls to 66% of peak value within 20 ns. According to the exponential fitting in nonlinear part, the current decay function can be defined as $I = -0.0019 + 0.016 \exp(-t/16.8)$. It can be seen that the fall time is about 17 ns which was faster than the previous reports [19–21]. The slow response is usually attributed to the oxygen adsorption at the surface and grain boundaries [22,23]. On the ZnO surface, the trapping can be easily induced, which can lead to the oxygen adsorption at the interface of Pt/ZnO film when exposed to air. Therefore, we attribute our faster process to the reduction of interface states which may result from our novel device structure.

4. Conclusion

ZnO films with high crystallinity were grown by PLD on Pt/Ti buffer layer, forming Schottky contacts. The post-annealing was found important to improve the crystallinity, uniformity of ZnO films and suppress the native defects related to oxygen vacancy as well as enhance the rectification of Pt/ZnO films Schottky contacts. The Pt/ZnO Schottky diode with best rectification shows barrier height of 0.8 eV with reverse leakage current of 1.5×10^{-5} A/cm^2. The best Schottky diode shows the largest responsivity of 0.265 A/W under illumination of light at wavelength of 378 nm, and the fast photo-response component with a rise time of 10 ns and a fall time of 17 ns. This report clearly demonstrates that ZnO films/Pt hetero-junction with Schottky contact can be realized through deposition of ZnO films on Pt bottom electrode, and establishes the potential of this structure system for use in zero-biased UV photodetector devices.

References

[1] S.J. Pearton, D.P. Norton, K. Ip, Y.W. Heo, T. Steiner, J. Vac. Sci. Technol., B 22 (2004) 932.
[2] D.C. Look, Mater. Sci. Eng., B, Solid-State Mater. Adv. Technol. 80 (2001) 383.
[3] S.J. Pearton, D.P. Norton, K. Ip, Y.W. Heo, T. Steiner, Prog. Mater. Sci. 50 (2005) 293.
[4] R.D. Vispute, V. Talyansky, R.P. Sharma, Appl. Surf. Sci. 431 (1998) 127.
[5] Y.R. Ryu, T.S. Lee, H.W. White, J. Cryst. Growth 261 (2004) 502.
[6] A. Ohtomo, H. Kimura, K. Saito, J. Cryst. Growth 214 (215) (2000) 284.
[7] C.A. Mead, Phys. Lett. 18 (1965) 218.
[8] R.C. Neville, C.A. Mead, J. Appl. Phys. 41 (1970) 3795.
[9] J.C. Simpson, F. Cordaro, J. Appl. Phys. 63 (1988) 1781.
[10] N. Ohashi, J. Tanaka, T. Ohgaki, H. Haneda, M. Ozawa, T. Tsurumi, J. Mater. Res. 17 (2002) 1529.
[11] H. Sheng, S. Muthukumar, N.W. Emanetoglu, Y. Lu, Appl. Phys. Lett. 80 (2002) 2132.
[12] F.D. Auret, S.A. Goodman, M. Hayes, M.J. Legodi, H.A. van Laarhoven, Appl. Phys. Lett. 79 (2001) 3074;
F.D. Auret (private communication).
[13] B.J. Coppa, R.F. Davis, R.J. Nemanich, Appl. Phys. Lett. 82 (2003) 400.
[14] H. Yamada, Y. Ushimi, M. Takeuchi, Y. Yoshino, S. Arai, Vacuum 74 (2004) 689.
[15] T. Nagata, A. Ashida, N. Fujimara, T. Ito, J. Alloys Compd. 371 (2004) 157.
[16] B.T. Khuri-Yakub, J.G. Smits, T. Barbee, J. Appl. Phys. 52 (1981) 4772.
[17] R. Duclere a, C. Mc Loughlin a, J. Fryar, Thin Solid Films 500 (2006) 78.
[18] D.G. Thomas, J. Phys. Chem. Solids 3 (1957) 229.
[19] S. Liang, H. Sheng, Y. Liu, Z. Huo, Y. Lu, J. Cryst. Growth 225 (2001) 110–113.
[20] S.J. Young, L.W. Ji, T.H. Fang, S.J. Chang a, Acta Mater. 55 (2007) 329–333.
[21] D.Y. Jiang, Jiying Zhang, Youming Lu, Solid-State Electron. 52 (2008) 679–682.
[22] Y. Takahashi, M. Kanamori, A. Kondoh, Jpn. J. Appl. Phys. 33 (1994) 6611.
[23] D.H. Zhang, J. Phys. D 28 (1995) 1273.